**RESEARCH ARTICLE**

**Key Points:**
- We present new luminescence proxies for precipitation and compare them with well-established proxies from the same drainage basin
- The new proxies agree with long-chain $n$-alkane δD and bulk sediment ln (Fe/Ca) and correlate very well with modeled precipitation
- The luminescence proxies are based on quartz and feldspar, common components of terrigenous sediments

**Correspondence to:**
V. R. Mendes,
vrm.unifesp@gmail.com

# Thermoluminescence and Optically Stimulated Luminescence Measured in Marine Sediments Indicate Precipitation Changes Over Northeastern Brazil

**Vinícius R. Mendes[1,2]** [ID], **André O. Sawakuchi[1]** [ID], **Cristiano M. Chiessi[3]** [ID], **Paulo C. F. Giannini[1]**, **Kira Rehfeld[4]** [ID], and **Stefan Mulitza[5]** [ID]

[1]Luminescence and Gamma Spectrometry Laboratory (LEGaL), Department of Sedimentary Geology, University of São Paulo, São Paulo, Brazil, [2]Institute of Marine Science, Federal University of São Paulo, São Paulo, Brazil, [3]School of Arts, Sciences and Humanities, University of São Paulo, Santos, Brazil, [4]British Antarctic Survey, Cambridge, United Kingdom and Institute of Environmental Physics, Heidelberg University, Heidelberg, Germany, [5]MARUM-Center for Marine Environmental Sciences, University of Bremen, Bremen, Germany

**Abstract** Marine sediment cores offer a great number of proxies for reconstructions of past environmental conditions, such as ocean temperature, salinity, primary productivity, stratification of the upper water column, and continental precipitation. Up to date, continental precipitation archived in marine sediment cores is reconstructed based mainly on the hydrogen isotopic composition of plant-wax compounds (i.e., $n$-alkane δD) or on the ratio between terrigenous and marine sediments expressed as elemental ratios (e.g., ln (Fe/Ca)). Although these proxies provide reliable precipitation reconstructions, there are some inherent limitations, as plant-wax δD application depends on the availability of $n$-alkanes in marine sediments and elemental ratios can be influenced by other factors like the relative sea-level, primary productivity, and postdepositional processes. Here we introduce new precipitation proxies based on optically stimulated luminescence and thermoluminescence signals of quartz and feldspar. The rationale is that when precipitation changes over the catchment through time, different sediment sources regarding weathering intensity and parent rock types are drained, supplying sediments with varying signals of luminescence to the ocean. We compared our new proxy records with records of well-established proxies, for the same (ln (Fe/Ca)) and neighboring ($n$-alkane δD) marine sediment cores. The comparison among all proxies as well as with a state-of-art transient climate model run (TraCE-21ka) demonstrates that the new proxies accurately constrain precipitation changes over northeastern Brazil for the last 30,000 years. The main advantage of these new proxies relies on their fast response to precipitation changes over the continent. Furthermore, they are straightforward to measure and not expensive.

**Plain Language Summary** Deepwater marine sediments are constituted mostly from geological and biological fine materials that can be deposited without disturbance forming excellent archives of changes in environmental conditions. In this study, we analyzed a marine sediment core collected offshore Brazil's northeastern coast. In this marine sediment core, we can find clay minerals, quartz, and feldspar from the continent, mainly transported by the Parnaíba River—the most important river in the region. Any substantial change experienced by the river is potentially registered in the marine sediments. Here we propose a new way to reconstruct past changes in continental precipitation over northeastern Brazil. This new method is based in the luminescence of quartz and feldspar grains. These properties depend mostly on the geology of source areas where the grains came from and how long they have been submitted to surface processes. The comparison of our new method with well-established ones and with a state-of-the-art climate model output demonstrates that it can accurately constrain precipitation changes over northeastern Brazil for the last 30,000 years. When compared with previous methods, our new method shows significant improvements because it is less sensitive to variations in sea level, it is faster to obtain, and it is cost effective.

## 1. Introduction

Constraining basin-wide changes in continental precipitation (fluvial discharge) is of crucial importance to understand the response of rivers and forests to climatic changes. Reconstructions of changes in continental precipitation can be performed, for instance, through the hydrogen isotopic composition of plant-wax
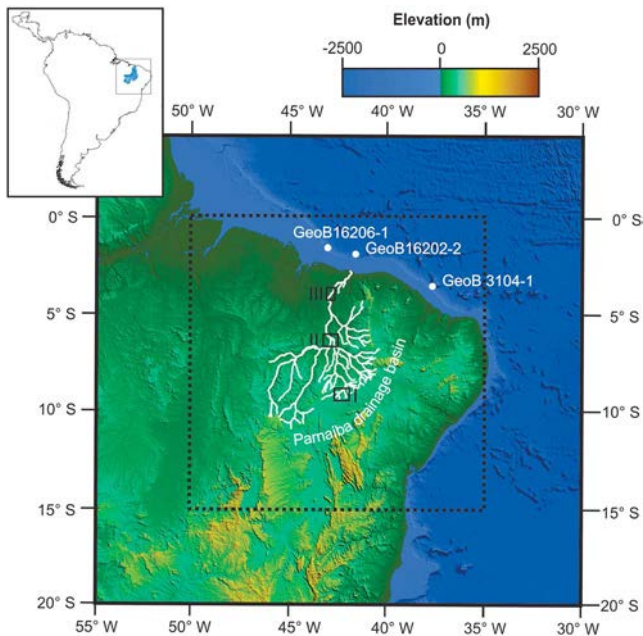
**Figure 1.** Digital elevation model (ETOPO1; Amante & Eakins, 2009) of northeastern South America and the adjacent Atlantic. The map shows the Parnaíba River drainage basin (white lines); the location of marine sediment cores GeoB3104-1 (Arz et al., 1998), GeoB16206-1 (Zhang et al., 2015; this study), and GeoB16202-2 (Mulitza et al., 2017; white circles); the area for simulated precipitation from the transient model run TraCE-21ka (Liu et al., 2009; black dashed rectangle); and the location of the continental samples (black rectangles: I—Porcos Lake; II and III—medium and low Parnaíba River, respectively).

compounds (*n*-alkane δD; e.g., Schefuß et al., 2005) and bulk sediment elemental ratios like ln (Fe/Ca; e.g., Arz et al., 1998). However, the application of plant-wax δD depends on the availability of *n*-alkanes in marine sediments (e.g., Häggi et al., 2016; Sauer et al., 2001) and elemental ratios can be influenced by other factors like sediment grain size, relative sea-level, primary productivity, and post-depositional processes (e.g., Clift et al., 2014; Govin et al., 2012). Therefore, new proxies based on major components of terrigenous sediments, like quartz and feldspar, would be valuable to improve paleoclimate reconstructions. Together with the preexistent and well-established ones, these new proxies could help to add additional information on continental erosional process and river flux to the ocean through time.

Here we introduce a new precipitation proxy based on luminescence signals of quartz and feldspar grains. Our precipitation proxy is based on the optically stimulated luminescence (OSL) and thermoluminescence (TL) sensitivities (emission intensity per unit mass per unit radiation dose) of quartz and feldspar grains deposited in marine settings. Particularly, OSL and TL sensitivities of quartz allow to track continental sediment sources (e.g., Zular et al., 2015) and are based on an abundant and resistant mineral, even under tropical weathering conditions. Pioneering studies about the luminescence of quartz (Huntley et al., 1985) and feldspar (Godfrey-Smith et al., 1988) supported the development of a well-established dating method to determine sediment burial ages for Quaternary sedimentary sequences (Buylaert et al., 2012; Murray & Wintle, 1998). In the recent years, the OSL and TL of quartz and feldspar provided the basis for new methods to study Earth surface processes, including surface exposure dating (Sohbati et al., 2012), estimation of Quaternary uplift rates in mountain building zones (King et al., 2016), and sediment provenance (Nian et al., 2019; Sawakuchi et al., 2012; Sawakuchi et al., 2018; Zular et al., 2015). Here we applied OSL and TL signals related to quartz and feldspar from marine sediment core GeoB16206-1 collected off northeastern South America (Figure 1) as proxies to track changes in precipitation. OSL and TL sensitivities were also measured in continental sediment samples to monitor the signatures of different areas sourcing sediments to our core site (Figure 1). The rationale is that changes in precipitation over the hydrologic basin could be reflected in the luminescence signal recorded in the marine sediment core. The increase of precipitation over the catchment could promote higher recycling cycles (burial and exposure), which is one the known factor of sensitivization of quartz. Another possible reason for sensitivity changes in marine sediments could be related to variations in sources of sediments, by varying the area of the catchment and promoting the expansion or retreat of headwaters. For example, the expansion of headwaters increases the distance of sediment transport as well as allow the input of sediments from different sources.

It was recently shown that TraCE-21ka could accurately reproduce changes in precipitation over northeastern Brazil during the last deglaciation (Bouimetarhan et al., 2018; Mulitza et al., 2017). Thus, despite its limitations (Liu et al., 2009), we compare our new TL and OSL luminescence proxies as well as the previously available records for the same core ((ln (Fe/Ca); Zhang et al., 2015) and for a neighboring core (*n*-alkane δD; Mulitza et al., 2017).

The studied sediment core received continental sediments from the Parnaíba River drainage basin (Figure 1; Zhang et al., 2015; Häggi et al., 2016), and the core records the last approximately 30 kyr, comprising major changes in precipitation over northeastern South America, like Heinrich stadials (HS) 2 and 1, the Younger Dryas (YD), Bond events, and the middle to late Holocene shift (Arz et al., 1998; Cruz et al., 2009; Prado et al., 2013; Zhang et al., 2015). Our data show that the OSL and TL signals of quartz and feldspar of sediments from the continental margin off northeastern South America can be successfully used as proxies for precipitation over the adjacent continent.
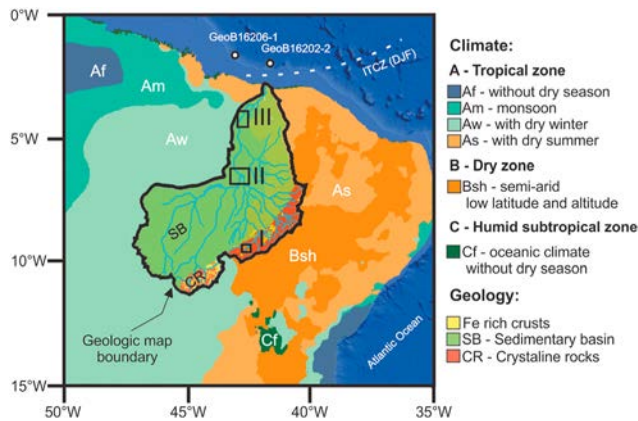
**Figure 2.** Köppen's climatic classification review (Alvares et al., 2013) for northeastern South America with a simplified geological map (area surrounded by the black line, adapted from CPRM, 2006) of the Parnaíba River drainage basin (main tributaries depicted by the blue lines) and the location of the continental samples (black rectangles: I—Porcos Lake; II and III— medium and low Parnaíba River, respectively). Most of the basin runs over sedimentary rocks, but some portions of the headlands comprise igneous and metamorphic rocks with Fe-rich crusts. Precipitation is mainly influenced by the Intertropical Convergence Zone southward shift by the end of austral summer (December-February, DJF).

## 2. Regional Setting

The Parnaíba River catchment is one of the major drainage basins in northeastern Brazil, covering three different climatic classes according to a review of Köppen's classification (Figure 2; Alvares et al., 2013): Bsh, semiarid; As, tropical with dry summer; and Aw, tropical with dry winter. Precipitation over northeastern South America is highly influenced by the meridional shifts of the Intertropical Convergence Zone (ITCZ) both on seasonal (Marengo & Bernasconi, 2015) and millennial timescales (Mulitza et al., 2017). Peak annual precipitation occurs during March/April when the ITCZ reaches its southernmost seasonal position (Hastenrath, 2012). On millennial timescales, slowdowns of the Atlantic Meridional Overturning Circulation during Northern Hemisphere cold events (i.e., Heinrich Stadials) triggered further southward shift of the ITCZ (Portilho-Ramos et al., 2017) and promoted increased precipitation over significant parts of northeastern South America to the south of the equator (Zhang et al., 2017). These enhanced precipitation periods were registered in speleothems (Stríkis et al., 2015; Wang et al., 2004) and marine sediment cores (Arz et al., 1998; Zhang et al., 2015).

Two main geologic units occur within the Parnaíba River drainage basin (Figure 2): (i) sedimentary rocks from the Parnaíba intracratonic sedimentary basin and (ii) igneous and metamorphic rocks from the Riacho do Pontal mobile belt. There is a widespread presence of Fe-rich crusts (ferricrets) covering soils over the headlands of the catchment (CPRM, 2006; Figure 2), suggesting past heavy weathering conditions.

## 3. Materials and Methods

### 3.1. Core Location, Chronology, and Reference Proxies

We investigated marine gravity core GeoB16206-1 (Table 1; Mulitza et al., 2013) collected off northeastern South America, 180 km offshore the Parnaíba River mouth (Figure 1). We used the age model established by Zhang et al. (2015) based on 12 $^{14}$C ages, obtained on samples of planktonic foraminifera *Globigerinoides sacculifer*. Raw radiocarbon ages were calibrated and linearly interpolated, and the resulting age model covers the last approximately 30 kyr (for details, see Zhang et al., 2015). Core GeoB16206-1 is ideally suited for developing the luminescence proxies not only because it covers the last three major millennial-scale events of increased precipitation over northeastern Brazil but also because two previous studies applied established proxies for continental rainfall (i.e., ln (Fe/Ca) and *n*-alkane δD) at the same (i.e., GeoB16206-1; Zhang et al., 2015) or a neighbor core (i.e., GeoB16202-2; Mulitza et al., 2017). Besides the downcore reconstructions of continental precipitation used as reference proxies, we also compare the results of our luminescence downcore records to the precipitation output of the transient model run TraCE-21ka (Liu et al., 2009).

Sediment samples (119 in total) were collected with a 10-ml syringe (1.7-cm diameter) every 10 cm from 800- to 100-cm core depth, and every 2 cm for the uppermost 100 cm. In the uppermost meter, about 250 years are integrated into one sample, samples in the lowermost 7 m contain approximately 50 years each one.

**Table 1**
*Marine Sediment Cores Cited and Used in This Study*

| Core (GeoB) | Coordinates | Water depth (m) | Length (m) |
|---|---|---|---|
| 3104-1 (Arz et al., 1998) | 3°40.09′S, 37°43.09′W | 767 | 5.2 |
| 16202-2 (Mulitza et al., 2017) | 1°54.50′S, 41°35.50′W | 2,248 | 7.6 |
| 16206-1 (Mulitza et al., 2013) | 1°34.75′S, 43°01.42′W | 1,367 | 8.1 |

**Table 2**
*Continental Sediment Samples and Used in This Study*

| Sample | Coordinates | Elevation (m) | Water depth (m) |
|---|---|---|---|
| PAR 01B | 6°16.463′S, 42°49.614′W | | 1.0 |
| PAR 02B | 6°16.338′S, 42°49.989′W | 93 | 1.5 |
| PAR 4B | 6°14.220′S, 42°51.807′W | 93 | 1.5 |
| PAR 5B | 6°16.215′S, 42°51.123′W | 95 | 1.0 |
| PAR 8A | 6°13.826′S,42°52.146′W | 91 | 3.6 |
| PAR 10A | 4°9.309′S, 42°54.665′W | 33 | 3.0 |
| PAR 11A | 4°9.300′S, 42°55.900′W | 38 | 1.0 |
| PAR 11B | 4°9.300′S, 42°55.900′W | 38 | 5.0 |
| PAR 15B | 3°53.755′S, 42°43.267′W | 27 | 3.5 |
| Porcos lake | 9°9.226′S, 42°38.994′W | 390 | - |

### 3.2. Parnaíba River Drainage Basin Samples

To obtain the luminescence characteristics of sediments sourced by the Parnaíba River, modern riverbed and buried lake sediments were collected and analyzed (Figures 1 and 2 and Table 2). Riverbed sediment samples (*n*=9) were collected with a van Veen grab sampler along the middle and lower portions of Parnaíba River during the flood season (February 2014; Figures 1 and 2I and 2II). Lake sediment samples (*n*=30) were collected from Porcos Lake, an ephemeral lake within the upper Parnaíba River catchment (December 2012). The lake samples were collected every 5 cm with 10-ml syringes along a 1.6-m-thick mud layer profile, exposed in the top of an 2.9-m depth archeological excavation, from which megafauna teeth Electron Spin Resonance dating provided ages spanning from 30 to 19 ka, which is the interval of maximum ages for the entire sedimentary deposit (Kinoshita et al., 2014). The age of the mud layer is based on two (bottom and top samples) accelerator mass spectrometry radiocarbon date (bulk organic matter), calibrated with the CALIB 7.1, using calibration curve "SHcal 13" (Stuiver et al., 2019)

### 3.3. Luminescence Measurements

All the samples were oven-dried at 60°C and precisely weighted to 0.5 g. Samples were treated with $H_2O_2$ 27% and HCl 10% to remove organic matter and carbonate ($CaCO_3$), respectively. Grains of heavy minerals or mica have an insignificant contribution to OSL and TL signals of quartz or feldspar measured in polymineral aliquots. This is supported by the low sensitivity of these minerals compared to the OSL and TL (UV emission) of quartz and feldspar (del Río et al., 2019; Krbetschek et al., 1997; Zular et al., 2015). After every chemical treatment step, samples were washed 2 times with distilled water to remove the chemical reagents. A centrifuge was used to accelerate the deposition of suspended material and improve silt and clay recuperation during the distilled water steps. Acetone was added to the remaining content until 5 ml. After homogenizing, three aliquots were mounted per sample using four drops of the acetone solution with sediments dropped in aluminum discs. Stokes settling time were used to ensure that only grains of silt and clay (<0.063 mm) were collected with the pipette used to mount the discs used for luminescence measurements

Luminescence measurements were performed on an automated Risø DA-20 TL/OSL reader with built-in $^{90}Sr/^{90}Y$ beta source (dose rate of 0.084 Gy/s), blue light-emitting diodes (470 nm), and infrared light-emitting diodes (870 nm) for stimulation and light detection in the ultraviolet band using Hoya U-340 filters (290–370 nm). Sample preparation and luminescence measurements were carried out in the Luminescence and Gamma Spectrometry Laboratory of the Institute of Geosciences, University of São Paulo, Brazil. The measurement protocol was adapted from protocols suggested by Zular et al. (2015) and Sawakuchi et al. (2018) to measure luminescence sensitivity (intensity of emitted light per unit mass per unit radiation dose) related to quartz and feldspar grains from polymineral aliquots. Table 3 shows the protocol used in this study for luminescence measurements. Here, we refer to OSL as the light emission when

**Table 3**
*Protocol Used to Measure OSL and TL 110°C (Thermoluminescence) Sensitivities and IRSL/OSL Ratio*

| Step | Procedure |
|---|---|
| 1 | IR stimulation for 100 s at 125°C |
| 2 | Blue light stimulation for 100 s at 125°C |
| 3 | Dose of 30 Gy |
| 4 | IR stimulation for 100 s at 50°C |
| 5 | Blue stimulation for 100 s at 125°C |
| 6 | Blue stimulation for 100 s at 125°C |
| 7 | TL until 250°C at 5°C/s |
| 8 | Dose of 30 Gy |
| 9 | TL until 250°C at 5°C/s |
| 10 | TL until 250°C at 5°C/s |

Abbreviations: IRSL, infrared stimulated luminescence; OSL: optically stimulated luminescence; TL: thermoluminescence.
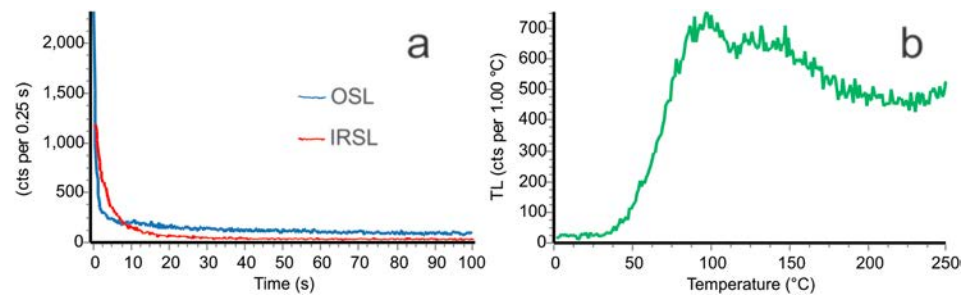
**Figure 3.** Examples of (a) infrared stimulated luminescence (IRSL, red curve) and optically stimulated luminescence (OSL, blue curve) decay curves and (b) thermoluminescence (TL, green curve) glow curve measured in steps 4, 5, and 7, respectively, of the protocol described in Table 3.

polymineral aliquots are stimulated with blue light. Infrared stimulated luminescence (IRSL) at 125°C was used before every OSL measurement to minimize the contribution of feldspar signals on the quartz OSL signal (Wallinga et al., 2002). This procedure allows measuring a quartz-dominated signal in polymineral aliquots (Sawakuchi et al., 2018). The TL signal was measured until 250°C to prevent major sensitivity changes (Wintle & Murray, 2000) and keep the natural luminescence characteristics of the samples. The 30-Gy dose was defined to be high enough to permit measurable OSL and TL signals in the studied polymineral aliquots and to avoid a significant change in the natural sensitivity of the sample. The integral of the first second of the OSL decay curve normalized by the total OSL (0–100 s) was used to represent a fast-component dominated signal of quartz (Jain et al., 2003). The TL signal was obtained integrating the TL curve from 80 to 120°C minus the background and normalized by the integral of the entire TL curve (0–250°C; Figure 3). The TL signal in the 80–120°C range is considered to ensure the measurement of the sensitivity of the TL 110°C peak with a heating rate of 5°C/s, which is attributed to quartz (Petrov & Bailiff, 1995). The OSL and TL sensitivities were obtained as the mean of the three aliquots measured per sample and the standard deviation were used to evaluate the variability among aliquots of each sample (Table S1). The IRSL/OSL ratio was also calculated to measure the concentration of feldspar in relation to quartz (Duller, 2003; Sawakuchi et al., 2018). The IRSL signal was calculated as the integral of the first second of light emission and considering the last ten seconds as background (Table S1).

### 3.4. Cross-Correlation Analysis

The Pearson correlation coefficient was estimated for the correlation between proxies (proxy-to-proxy comparison) and proxies with modeled precipitation (proxy-to-model correlation). The correlation estimates between cores respect the uneven sampling (Rehfeld et al., 2011; Rehfeld & Kurths, 2014) and p-values were corrected for lag-1 autocorrelation (Zwiers & Von Storch, 1995). The correlations were estimated on two different timescales. The first one comprises the entire timescale and contains the deglacial trend. This scale allows the evaluation of the proxies' response to long-term changes. For the second timescale (detrended), the deglacial trend was removed with a 3,000-year Gaussian smoother. This scale targets the millennial to centennial changes and is more affected by proxy noise and age uncertainty. The detrending was applied to all variables. Choosing a 3,000-year window (as, e.g., in Rehfeld & Laepple, 2016) for the smoother separates out the orbital signal (which dominates the correlation results for the untreated analysis) and retains centennial to millennial variability. At these timescales, age model uncertainty (on the x-axis, in the order of centuries) and proxy noise (on the y-axis) have a relatively stronger impact on the correlation results than for the orbital timescale that includes the general deglaciation trends (Rehfeld & Kurths, 2014). Thus, at the centennial to millennial timescale the correlations are not significant, or as strong as on orbital timescales. We are interested in proxies that can give insights on as many timescales as possible, ideally at the minimum timescale the resolution of the core allows. Therefore, studying the centennial-to-millennial scale is important, even if the correlation is not as strong as the orbital scale.

## 4. Results

Core GeoB16206-1 luminescence results show increased OSL and TL sensitivities during periods of enhanced precipitation over northeastern Brazil (i.e., HS2, HS1, YD, and Bond events) as the IRSL/OSL
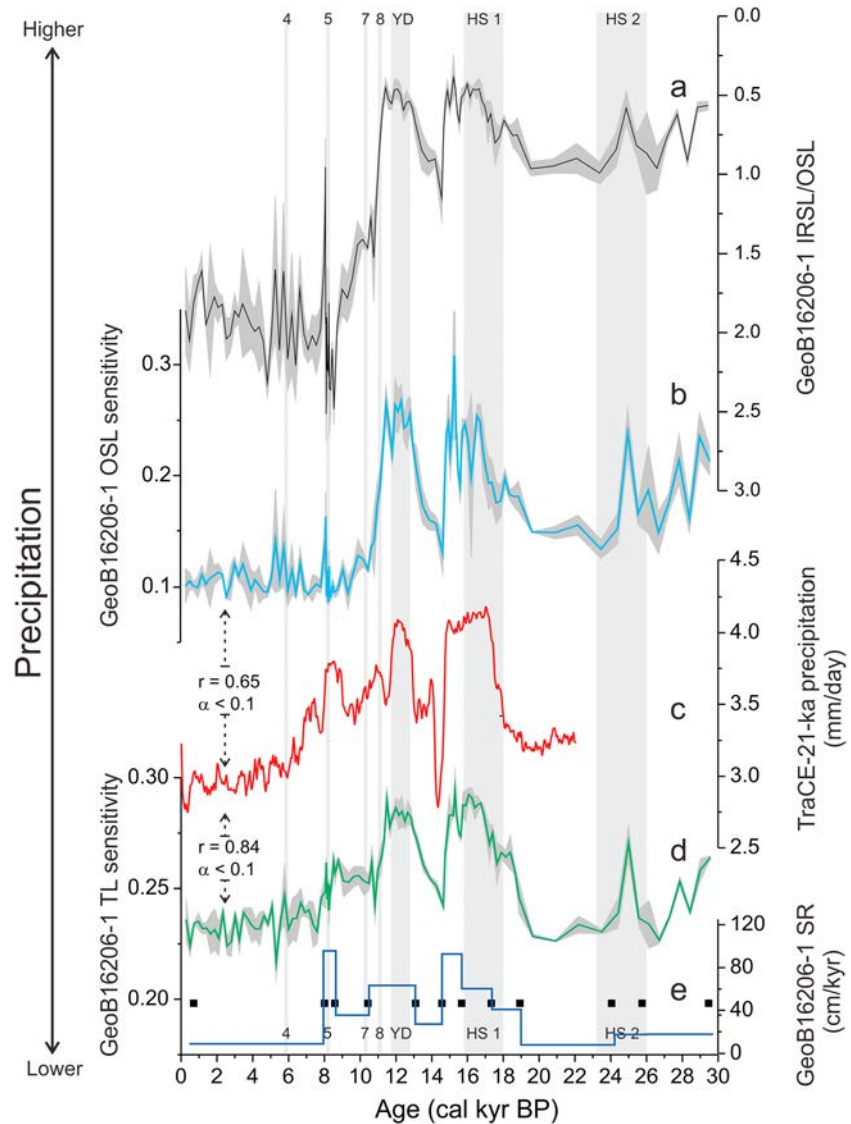
**Figure 4.** Downcore variability of the luminescence results of marine sediment core GeoB16206-1 and their relation with modeled precipitation and sedimentation rate. (a) Infrared/optically stimulated luminescence ratio (IRSL/OSL, inverted scale), indicating the feldspar-to-quartz concentration. (b) OSL sensitivity represented by the proportion of the first second of light emission over the total emission (1–100 s). (c) Modeled precipitation over northeastern Brazil (TraCE-21ka, Liu et al., 2009); the specific area is shown in Figure 1. (d) TL (thermoluminescence) sensitivity representative of the 110°C TL peak (TL emission from 80 to 120°C). (e) Sedimentation rates (Zhang et al., 2015). The black squares show calibrated ^{14}C ages used to build the age model of core GeoB16206-1 (Zhang et al., 2015). The gray shading in a, b, and d indicates the standard deviation for luminescence results. Pearson correlation coefficient reinforces the visual impression that TL sensitivity signal better fits the TraCE-21ka prediction than OSL sensitivity, with $r = 0.84$ and $r = 0.65$, respectively, both of them with significance level higher than 0.1. The proxies show enhanced precipitation during Heinrich stadials (HS1 and HS2), the Younger Dryas (YD), and Bond events (8-4; grey vertical bars) with a gradual decrease in precipitation along the Holocene.

values decrease (Figures 4a, 4b, and 4d). Both OSL and TL sensitivities curves vary in the same way during the studied period; if we exclude the high-frequency variations, higher IRSL/OSL is related with lower OSL and TL sensitivities (Figures 4a, 4b, and 4d). The TL sensitivity shows a higher correlation than OSL sensitivity (respectively, $r = 0.84$ and $r = 0.65$, both $\alpha < 0.1$) with the modeled precipitation for northeastern Brazil including the Parnaíba River drainage basin (TraCE-21ka; Liu et al., 2009; Figures 4c and 5). However, the OSL sensitivity shows a higher correlation than TL sensitivity with the δD (Figure 5; respectively, $r = -0.39$ and $r = -0.34$, both $\alpha < 0.1$). Considering the detrended correlation (Figure 5, lower triangle), only the TL
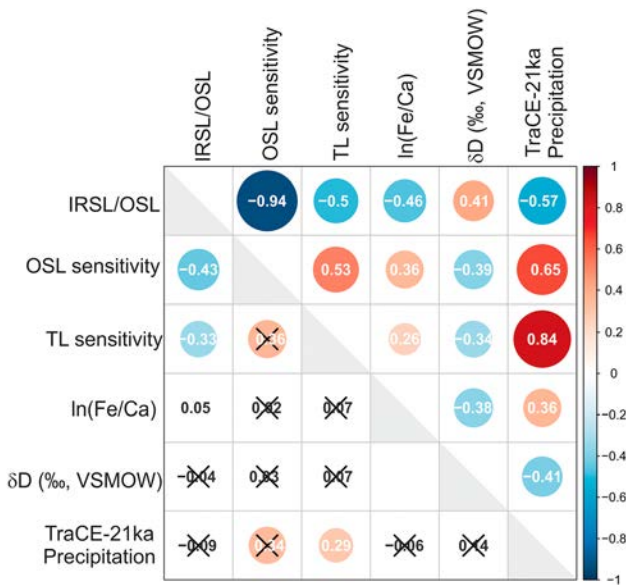
sensitivity correlates significantly with other proxies. Periods of higher OSL and TL sensitivities are related to higher sedimentation rates at the site of core GeoB16206-1 (Figures 4b, 4d, and 4e).

Although there is a small overlap of values, there is a clear trend of increasing TL sensitivity from the marine sediment core (lower values) to riverbed sediment of middle and downstream sectors of the Parnaíba River (intermediate values) and to sediment of the ephemeral lake at the headland of the Parnaíba River drainage basin (higher values; Figure 6). This pattern is better observed when statistics (quartiles and median values) of each sediment source unit are compared.

The samples from Porcos Lake comprise almost the entire Holocene Table 4, as the Parnaíba river samples represent the present-day sedimentary conditions.



**Figure 5.** Correlation matrix with 90% confidence intervals (crossed values are below this interval) for the original (upper triangle) and the detrended (lower triangle) records. Time series used to calculate the correlation in the lower triangle were detrended with a 3,000-year Gaussian smoother. The circle size and colors also indicate the correlation index values. Infrared stimulated luminescence (IRSL), optically stimulated luminescence (OSL), and thermoluminescence (TL) are the luminescence proxies (this study). Previously available precipitation proxies for the same drainage basin include ln (Fe/Ca; Zhang et al., 2015) and δD (‰, VSMOW; Mulitza et al., 2017). TraCE-21ka is the modeled precipitation for northeastern Brazil, including the Parnaíba River drainage basin (Liu et al., 2009).

## 5. Discussion

The suspension load of the Parnaíba River drainage basin is the primary source of terrigenous sediments deposited at the site of core GeoB16206-1 (Häggi et al., 2016; Zhang et al., 2015). Thus, downcore changes in luminescence sensitivity most likely stem from differences in suspension load through time. The concentration of feldspar grains (IRSL/OSL ratio) reduces, and the quartz OSL and TL sensitivities increase during periods of higher precipitation (Figure 7). Thus, high precipitation events promote the transfer of sediments with low feldspar content (low IRSL/OSL ratio) and high OSL and TL sensitivities to the ocean. Luminescence sensitivity was successfully used to identify different quartz and feldspar sources in suspended sediments of Amazonian rivers, where quartz sensitivity is controlled by the tectonic context of the source area (Sawakuchi et al., 2018). For the Amazonian rivers, one of the main factors that control sensitivity is the denudation rate of sediment sources. Quartz grains from the Andes, where higher denudation rates promote shorter residence time of quartz in soils, show lower sensitivity when compared to quartz grains from cratonic shield areas (lower denudation rates and more prolonged weathering; Sawakuchi et al., 2018). A similar rationale can be applied to the Parnaíba River drainage basin not in terms of tectonics, but in terms of weathering time of the sediments sourced to the drainages. In the case of Parnaíba River catchment, periods of lower precipitation implied lower denudation rates and longer residence time of mineral particles in soil profiles drained by headwaters and/or within the fluvial system before transport to marine settings. The difference between the TL and OSL sensitivity curves can be attributed to the influence of feldspar contamination on the OSL signal, which is higher during the Holocene (higher IRSL/OSL ratio; Figure 4a). In this case, the IRSL treatment applied before the blue-light stimulation was unsuitable for complete depletion of feldspar OSL in Holocene samples rich in feldspar. The contribution of sediments with higher OSL and TL sensitivities increases during wet periods like the HS2, HS1, and YD. This can be attributed to the expansion of the headwaters of the Parnaíba River basin. In this case, the headlands of the Parnaíba River drainage basin, which has the driest climate of Brazil (Bsh semi-arid; Alvares et al., 2013; Figure 2), would be connected with Parnaíba River main stem during wet periods, providing sediments with high luminescence sensitivity (Figure 6). This is in accordance with previous studies (Moska &
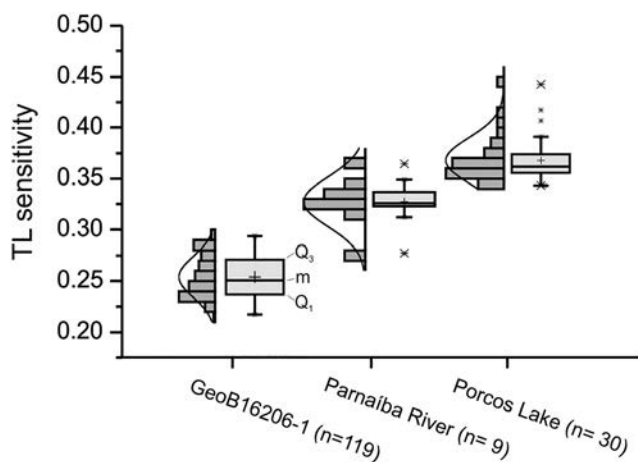


**Figure 6.** Boxplots and histograms of thermoluminescence (TL) sensitivity values obtained in samples of the marine sediment core GeoB16206-1 (lower values), riverbed sediments of the Parnaíba River (intermediate values), and sediments of the ephemeral Porcos Lake (higher values) in the headlands of the Parnaíba River drainage basin. Besides the small overlap, the boxplots (quartiles and median) of TL values clearly distinguish the units under comparison.

**Table 4**
*$^{14}C$ ages (AMS) for the Porcos lake mud layer*

| Sample | Depth (m) | Conventional age | Calibrated |
|--------|-----------|------------------|------------|
| P01 | 1.65 | 11,610 ± 70 BP | 13,434.5 ± 134.5 cal BP |
| P30 | 0.20 | 875 ± 35 BP | 876 ± 33 cal BP |

Abbreviations: AMS, accelerator mass spectrometry; BP, before present; cal BP, calibrated before present.

Murray, 2006; Pietsch et al., 2008) that recognized the luminescence sensitization of quartz as result of surface processes (light exposure during transport and irradiation during burial). We suggest that during periods with increased precipitation, this highly luminescence-sensitive quartz grains are carried to our core site, elevating the OSL and TL sensitivity of the core sediments. Importantly, high sensitivity values occur coevally with high ln (Fe/K; Figure 7a) values (Mulitza, 2012) from the same sediment core. Fe-rich deposits and rocks are common at the headlands of the Parnaíba River drainage basin (CPRM, 2006; Figure 2) and support the increased contribution of this portion of the basin during wet periods. Higher concentration of Fe in sediments with high OSL sensitivity is also observed in the Amazon River basin (Sawakuchi et al., 2018). Therefore, continental sediment sources exposed to longer weathering are enriched in Fe-oxide/hydroxide minerals and higher sensitivity quartz and they are fast eroded during wetter conditions, when vast amounts
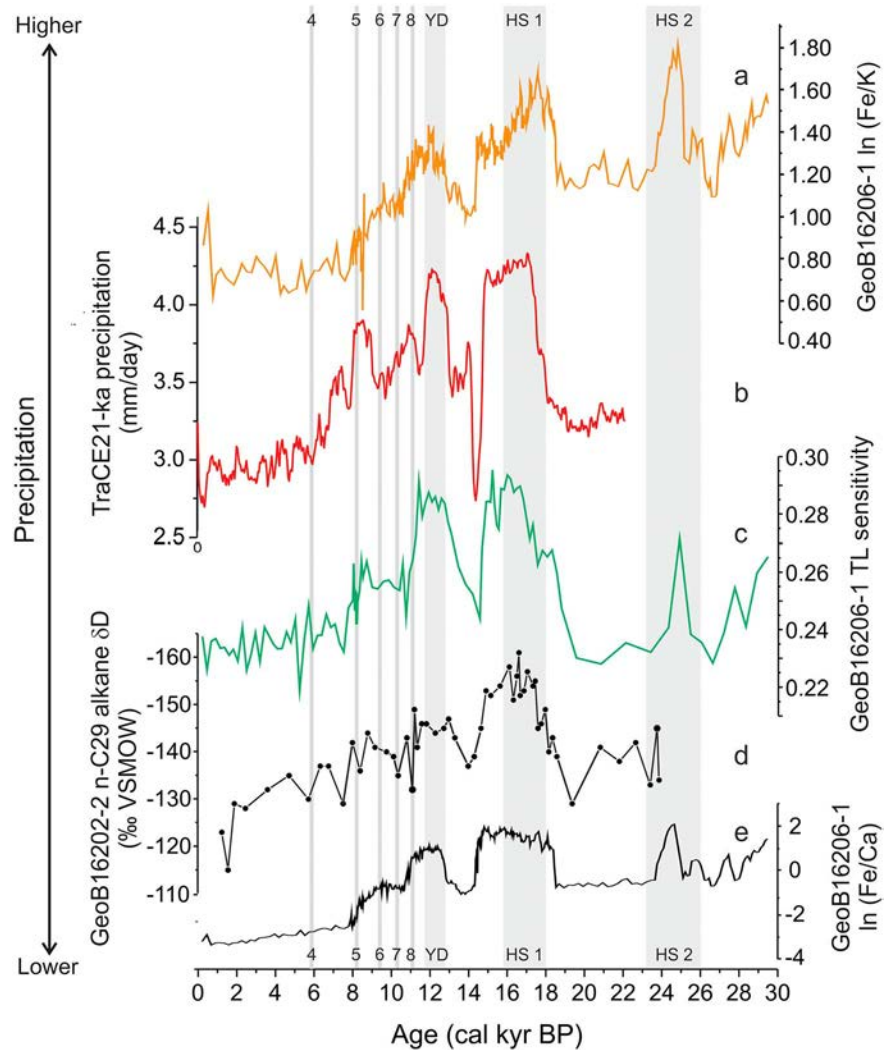


**Figure 7.** (a) Uncalibrated Fe/K record from marine sediment core GeoB16206-1 (Mulitza, 2012). (b) Modeled precipitation over northeastern Brazil (TraCE-21ka, Liu et al., 2009). The specific area is shown in Figure 1. (c) Thermoluminescence (TL) sensitivity from marine sediment core GeoB16206-1 (this study). (d) Ice volume corrected δD record of the n-C29 alkane of terrestrial plant-wax from marine sediment core GeoB16202-2 (Mulitza et al., 2017). (e) ln (Fe/Ca) record from marine sediment core GeoB16206-1 (Zhang et al., 2015). The grey vertical bars show Heinrich stadials (HS) 2 and 1, the Younger Dryas (YD), and Bond events 8–4.

of sediments are transported to the equatorial Atlantic, as demonstrated by the elevated sedimentation rates during stadial events (Zhang et al., 2015; Figure 4).

Core GeoB16206-1 covers the three most recent glacial increases in terrigenous discharge recorded off northeastern Brazil, namely, HS2, HS1, and the YD (Arz et al., 1998; Zhang et al., 2015). These three periods are characterized by elevated ln (Fe/Ca) values and sedimentation rates compared to the Last Glacial Maximum and the Holocene (Figures 5 and 7). Our luminescence records constrain not only these three well-known events of increased precipitation over northeastern Brazil (Cruz et al., 2009; Stríkis et al., 2015; Wang et al., 2004) but also some minor events during the Holocene, which could correspond to those reported in stable oxygen isotope records from South American speleothems, as the 8.2-ka event (Cheng et al., 2009).

Cross validation is crucial to improve confidence in new proxies. In general, our TL sensitivity curve agrees with proxies from the same (ln (Fe/Ca)) and nearby cores (*n*-alkane δD), respectively GeoB16206-1 (Zhang et al., 2015) and GeoB16202-2 (Mulitza et al., 2017; Figures 7e and 7d). The ln (Fe/Ca) record indicates the terrigenous versus marine biogenic input to the core site (Arz et al., 1998; Govin et al., 2012; Zhang et al., 2015). Thus, it depends not only on precipitation over the drainage basin but also on the marine carbonate productivity and dissolution and also on relative sea level (RSL; Govin et al., 2012). During the Last Glacial Maximum, RSL was approximately 130 m lower than preindustrial levels (Yokoyama et al., 2000), causing an offshore migration of the Parnaíba River mouth of more than 100 km, considering regional bathymetry. Despite these possible interferences, the ln (Fe/Ca) record from core GeoB16206-1 (Figure 7e; Zhang et al., 2015) allows the determination of the time and duration of increased continental precipitation intervals, but due to the high RSL variation it cannot be used to assess the relative amplitude of changes in precipitation. Variations in *n*-alkane δD over northeastern South America are primarily driven by changes in rainfall amount (Dansgaard, 1964; Häggi et al., 2016; Mulitza et al., 2017), so the δD of the water (and subsequently of *n*-alkanes) decreases as precipitation increases (Figure 7d). Thus, *n*-alkane δD is inversely related to the amount of precipitation.

Our luminescence proxies (IRSL/OSL ratio and OSL and TL sensitivities) roughly agree with *n*-alkane δD from neighboring core GeoB16202-2 ($r = 0.41$, $-0.39$ and $-0.37$, respectively; Mulitza et al., 2017; Figures 5 and 7). Among the three luminescence signals we have tested, the TL sensitivity proxy has the better correlation with TraCE-21ka modeled precipitation ($r = 0.84$; Figure 5), which could be related to a smaller influence of feldspar in TL 110° peak when compared to LOE first second. The TL sensitivity proxy can record less profound changes in precipitation such as minor events during the Holocene (i.e., 8.2-ka event; Figure 7c) that are recognized in speleothem records over the continent (Cheng et al., 2009). Thus, the fact that the new TL proxy shows a more direct linear response to precipitation when compared with previously available proxies could be related to the intensification of sediment transport and recycling processes due to increased humidity and fluvial activity. Finally, the TL proxy has the great advantage of being based on quartz grains, which are very abundant and resistant to weathering and postdepositional process.

## 6. Conclusions

The comparison between our new precipitation proxies based on the luminescence signals of quartz and feldspar on the one hand and previously available proxies (i.e., plant-wax *n*-alkane δD and bulk sediment ln (Fe/Ca)) and model outputs (i.e., TraCE-21ka) for the same drainage basin shows that the new proxies accurately record changes in precipitation over northeastern Brazil throughout the last 30,000 years. The main advantage of the new proxies relies on their fast response to changes in precipitation. Additionally, the relatively easy and fast measurements ensure higher resolution compared to plant-wax *n*-alkane δD, allowing to constrain high-frequency precipitation events. Among all tested precipitation proxies, the TL sensitivity has the best correlation with modeled precipitation ($r = 0.84$). Another advantage is that the TL sensitivity proxy would be robust to postdepositional changes because it is based on quartz, which is an abundant and resistant mineral.

## References

Alvares, C. A., Stape, J. L., Sentelhas, P. C., De Moraes Gonçalves, J. L., & Sparovek, G. (2013). Köppen's climate classification map for Brazil. *Meteorologische Zeitschrift*, *22*(6), 711–728. https://doi.org/10.1127/0941-2948/2013/0507

Amante, C., & Eakins, B. W. (2009). ETOPO1 1 Arc-minute global relief model: Procedures, data sources and analysis. NOAA Technical Memorandum NESDIS NGDC-24. https://doi.org/10.1594/PANGAEA.769615

Arz, H. W., Pätzold, J., & Wefer, G. (1998). Correlated millennial-scale changes in surface hydrography and terrigenous sediment yield inferred from Last-Glacial marine deposits off northeastern Brazil. *Quaternary Research*, *50*(2), 157–166. https://doi.org/10.1006/qres.1998.1992

Bouimetarhan, I., Chiessi, C. M., González-Arango, C., Dupont, L., Voigt, I., Prange, M., & Zonneveld, K. (2018). Intermittent development of forest corridors in northeastern Brazil during the last deglaciation: Climatic and ecologic evidence. *Quaternary Science Reviews*, *192*, 86–96. https://doi.org/10.1016/j.quascirev.2018.05.026

Buylaert, J. P., Jain, M., Murray, A. S., Thomsen, K. J., Thiel, C., & Sohbati, R. (2012). A robust feldspar luminescence dating method for Middle and Late Pleistocene sediments. *Boreas*, *41*(3), 435–451. https://doi.org/10.1111/j.1502-3885.2012.00248.x

Cheng, H., Fleitmann, D., Edwards, R. L., Wang, X., Cruz, F. W., Auler, A. S., et al. (2009). Timing and structure of the 8.2. kyr B.P. event inferred from δ 18O records of stalagmites from China, Oman, and Brazil. *Geology*, *37*(11), 1007–1010. https://doi.org/10.1130/G30126A.1

Clift, P. D., Wan, S., & Blusztajn, J. (2014). Reconstructing chemical weathering, physical erosion and monsoon intensity since 25 Ma in the northern South China Sea: A review of competing proxies. *Earth-Science Reviews*, *130*, 86–102. https://doi.org/10.1016/j.earscirev.2014.01.002

CPRM (2006). Companhia de Pesquisa e Recursos Minerais (Serviço Geológico do Brasil)/Ministério de Minas e Energia – Secretaria de Geologia, Mineração e Transformação Mineral. Mapa geológico do Estado do Piauí 1:1.000.000. Piauí.

Cruz, F. W., Vuille, M., Burns, S. J., Wang, X., Cheng, H., Werner, M., et al. (2009). Orbitally driven east-west antiphasing of South American precipitation. *Nature Geoscience*, *2*(3), 210–214. https://doi.org/10.1038/ngeo444

Dansgaard, W. (1964). Stable isotopes in precipitation. *Tellus*, *16*(4), 436–468. https://doi.org/10.3402/tellusa.v16i4.8993

del Río, I., Sawakuchi, A. O., Giordano, D., Mineli, T. D., Nogueira, L., Abed, T., & Atencio, D. (2019). Athermal stability, bleaching behavior and dose response of luminescence signals from almandine and kyanite. *Ancient TL*, *37*(1), 11–21.

Duller, G. A. T. (2003). Distinguishing quartz and feldspar in single grain luminescence measurements. *Radiation Measurements*, *37*(2), 161–165. https://doi.org/10.1016/S1350-4487(02)00170-1

Godfrey-Smith, D. I., Huntley, D. J., & Chen, W. H. (1988). Optical dating studies of quartz and feldspar sediment extracts. *Quaternary Science Reviews*, *7*(3-4), 373–380. https://doi.org/10.1016/0277-3791(88)90032-7

Govin, A., Holzwarth, U., Heslop, D., Ford Keeling, L., Zabel, M., Mulitza, S., et al. (2012). Distribution of major elements in Atlantic surface sediments (36°N–49°S): Imprint of terrigenous input and continental weathering. *Geochemistry, Geophysics, Geosystems*, *13*, Q01013. https://doi.org/10.1029/2011GC003785

Häggi, C., Sawakuchi, A. O., Chiessi, C. M., Mulitza, S., Mollenhauer, G., Sawakuchi, H. O., et al. (2016). Origin, transport and deposition of leaf-wax biomarkers in the Amazon Basin and the adjacent Atlantic. *Geochimica et Cosmochimica Acta.*, *192*, 149–165. https://doi.org/10.1016/j.gca.2016.07.002

Hastenrath, S. (2012). Exploring the climate problems of Brazil's Nordeste: A review. *Climatic Change*, *112*(2), 243–251. https://doi.org/10.1007/s10584-011-0227-1

Huntley, D. J., Godfrey-Smith, D. I., & Thewalt, M. L. W. (1985). Optical dating of sediments. *Nature*, *313*(5998), 105–107. https://doi.org/10.1038/313105a0

Jain, M., Murray, A. S., & Bøtter-Jensen, L. (2003). Characterisation of blue-light stimulated luminescence components in different quartz samples: Implications for dose measurement. *Radiation Measurements.*, *37*(4-5), 441–449. https://doi.org/10.1016/S1350-4487(03)00052-0

King, G. E., Herman, F., & Guralnik, B. (2016). Northward migration of the eastern Himalayan syntaxis revealed by OSL thermochronometry. *Science*, *353*(6301), 800–804. https://doi.org/10.1126/science.aaf2637

Kinoshita, A., Mayer, E., Mendes, V. R., Figueiredo, A. M. G., & Baffa, O. (2014). Electron spin resonance dating of megafauna from Lagoa dos porcos, Piau?, Brazil. *Radiation Protection Dosimetry*, *159*(1–4), 212–219. https://doi.org/10.1093/rpd/ncu178

Krbetschek, M. R., Götze, J., Dietrich, A., & Trautmann, T. (1997). Spectral information from minerals relevant for luminescence dating. *Radiation Measurements*, *27*(5-6), 695–748. https://doi.org/10.1016/S1350-4487(97)00223-0

Liu, Z., Otto-Bliesner, B. L., He, F., Brady, E. C., Tomas, R., Clark, P. U., et al. (2009). Transient simulation of last deglaciation with a new mechanism for bolling-allerod warming. *Science*, *325*(5938), 310–314. https://doi.org/10.1126/science.1171041

Marengo, J. A., & Bernasconi, M. (2015). Regional differences in aridity/drought conditions over Northeast Brazil: present state and future projections. *Climatic Change*, *129*(1-2), 103–115. https://doi.org/10.1007/s10584-014-1310-1

Moska, P., & Murray, A. S. (2006). Stability of the quartz fast-component in insensitive samples. *Radiation Measurements*, *41*(7-8), 878–885. https://doi.org/10.1016/j.radmeas.2006.06.005

Mulitza, S. (2012). X-ray fluorescence wet sample measurements of MSM20/3 sediment core GeoB16206-1. MARUM - Center for Marine Environmental Sciences, University Bremen, PANGAEA, doi: https://doi.org/10.1594/PANGAEA.785985

Mulitza, S., C. M. Chiessi, A. P. S. Cruz, T. Frederichs, J. G. Gomes, M. H. D. C. Gurgel, et al. (2013). Response of Amazon sedimentation to deforestation, land use and climate variability—Cruise No. MSM20/3—February 19–March 11, 2012—Recife (Brazil)—Bridgetown (Barbados), 86 pp., DFG-Senatskommission für Ozeanographie, Bremen.

Mulitza, S., Chiessi, C. M., Schefuß, E., Lippold, J., Wichmann, D., Antz, B., et al. (2017). Synchronous and proportional deglacial changes in Atlantic meridional overturning and northeast Brazilian precipitation. *Paleoceanography*, *32*, 622–633. https://doi.org/10.1002/2017PA003084

Murray, A. S., & Wintle, A. G. (1998). Factors controlling the shape of the OSL decay curve in quartz. *Radiation Measurements*, *29*(1), 65–79. https://doi.org/10.1016/S1350-4487(97)00207-2

Nian, X., Zhang, W., Qiu, F., Qin, J., Wang, Z., Sun, Q., et al. (2019). Luminescence characteristics of quartz from Holocene delta deposits of the Yangtze River and their provenance implications. *Quaternary Geochronology*, *49*, 131–137. https://doi.org/10.1016/j.quageo.2018.04.010

Petrov, S. A., & Bailiff, I. K. (1995). The "110°C" TL peak in synthetic quartz. *Radiation Measurements*, *24*(4), 519–523. https://doi.org/10.1016/1350-4487(95)00002-V

Pietsch, T. J., Olley, J. M., & Nanson, G. C. (2008). Fluvial transport as a natural luminescence sensitiser of quartz. *Quaternary Geochronology*, *3*(4), 365–376. https://doi.org/10.1016/j.quageo.2007.12.005

Portilho-Ramos, R. C., Chiessi, C. M., Zhang, Y., Mulitza, S., Kucera, M., Siccha, M., et al. (2017). Coupling of equatorial Atlantic surface stratification to glacial shifts in the tropical rainbelt. *Scientific Reports*, *7*(1). https://doi.org/10.1038/s41598-017-01629-z

Prado, L. F., Wainer, I., Chiessi, C. M., Ledru, M. P., & Turcq, B. (2013). A mid-Holocene climate reconstruction for eastern South America. *Climate of the Past*, *9*(5), 2117–2133. https://doi.org/10.5194/cp-9-2117-2013

Rehfeld, K., & Kurths, J. (2014). Similarity estimators for irregular and age-uncertain time series. *Climate of the Past*, *10*(1), 107–122. https://doi.org/10.5194/cp-10-107-2014

Rehfeld, K., Marwan, N., Heitzig, J., & Kurths, J. (2011). Comparison of correlation analysis techniques for irregularly sampled time series. *Nonlinear Processes in Geophysics*, *18*(3), 389–404. https://doi.org/10.5194/npg-18-389-2011

Rehfeld, K., & Laepple, T. (2016). Warmer and wetter or warmer and dryer? Observed versus simulated covariability of Holocene temperature and rainfall in Asia. *Earth and Planetary Science Letters*, *436*, 1–9. https://doi.org/10.1016/j.epsl.2015.12.020

Sauer, P. E., Eglinton, T. I., Hayes, J. M., Schimmelmann, A., & Sessions, A. L. (2001). Compound-specific D/H ratios of lipid biomarkers from sediments as a proxy for environmental and climatic conditions. *Geochimica et Cosmochimica Acta*, *65*(2), 213–222. https://doi.org/10.1016/S0016-7037(00)00520-2

Sawakuchi, A. O., Guedes, C. C. F., DeWitt, R., F. Giannini, P. C., Blair, M. W., Nascimento, D. R., & Faleiros, F. M. (2012). Quartz OSL sensitivity as a proxy for storm activity on the southern Brazilian coast during the Late Holocene. *Quaternary Geochronology*, *13*, 92–102. https://doi.org/10.1016/j.quageo.2012.07.002

Sawakuchi, A. O., Jain, M., Mineli, T. D., Nogueira, L., Bertassoli, D. J. Jr., Häggi, C., et al. (2018). Luminescence of quartz and feldspar fingerprints provenance and correlates with the source area denudation in the Amazon River basin. *Earth and Planetary Science Letters*, *492*, 152–162. https://doi.org/10.1016/J.EPSL.2018.04.006

Schefuß, E., Schouten, S., & Schneider, R. R. (2005). Climatic controls on central African hydrology during the past 20,000 years. *Nature*, *437*(7061), 1003–1006. https://doi.org/10.1038/nature03945

Sohbati, R., Murray, A. S., Chapot, M. S., Jain, M., & Pederson, J. (2012). Optically stimulated luminescence (OSL) as a chronometer for surface exposure dating. *Journal of Geophysical Research*, *117*, B09202. https://doi.org/10.1029/2012JB009383

Stríkis, N. M., Chiessi, C. M., Cruz, F. W., Vuille, M., Cheng, H., de Souza Barreto, E. A., et al. (2015). Timing and structure of Mega-SACZ events during Heinrich Stadial 1. *Geophysical Research Letters*, *42*, 5477–5484A. https://doi.org/10.1002/2015GL064048

Stuiver, M., Reimer, P. J., & Reimer, R. W. 2019. CALIB 7.1 [WWW program] at http://calib.org, accessed 2019-2-10

Wallinga, J., Murray, A. S., Bøtter-Jensen, L., Horowitz, Y. S., & Oster, L. (2002). Measurement of the dose in quartz in the presence of feldspar contamination. *Radiation Protection Dosimetry*, *101*(1), 367–370. https://doi.org/10.1093/oxfordjournals.rpd.a006003

Wang, X., Auler, A. S., Edwards, R. L., Cheng, H., Cristalli, P. S., Smart, P. L., et al. (2004). Wet periods in northeastern Brazil over the past 210 kyr linked to distant climate anomalies. *Nature*, *432*(7018), 740–743. https://doi.org/10.1038/nature03067

Wintle, A. G., & Murray, A. S. (2000). Quartz OSL: Effects of thermal treatment and their relevance to laboratory dating procedures. *Radiation Measurements*, *32*(5-6), 387–400. https://doi.org/10.1016/S1350-4487(00)00057-3

Yokoyama, Y., Lambeck, K., De Deckker, P., Johnston, P., & Fifield, L. K. (2000). Timing of the Last Glacial Maximum from observed sea-level minima. *Nature*, *406*(6797), 713–716. https://doi.org/10.1038/35021035

Zhang, Y., Chiessi, C. M., Mulitza, S., Sawakuchi, A. O., Häggi, C., Zabel, M., et al. (2017). Different precipitation patterns across tropical South America during Heinrich and Dansgaard-Oeschger stadials. *Quaternary Science Reviews*, *177*, 1–9. https://doi.org/10.1016/j.quascirev.2017.10.012

Zhang, Y., Chiessi, C. M., Mulitza, S., Zabel, M., Trindade, R. I. F., Hollanda, M. H. B. M., et al. (2015). Origin of increased terrigenous supply to the NE South American continental margin during Heinrich Stadial 1 and the Younger Dryas. *Earth and Planetary Science Letters*, *432*, 493–500. https://doi.org/10.1016/j.epsl.2015.09.054

Zular, A., Sawakuchi, A. O., Guedes, C. C. F., & Giannini, P. C. F. (2015). Attaining provenance proxies from OSL and TL sensitivities: Coupling with grain size and heavy minerals data from southern Brazilian coastal sediments. *Radiation Measurements*, *81*, 39–45. https://doi.org/10.1016/j.radmeas.2015.04.010

Zwiers, F. W., & Von Storch, H. (1995). Taking serial correlation into account in tests of the mean. *Journal of Climate*, *8*(2), 336–351. https://doi.org/10.1175/1520-0442(1995)008<0336:TSCIAI>2.0.CO;2